ICCCM-JOURNAL OF SOCIAL SCIENCES AND HUMANITIES
2026; 5 (sp): 82-94
Published online 3 25 2026 (https://icccmjssh.com/) doi:
https://doi.org/10.53797/icccmjssh.v5isp.10.2026
e-ISSN 2811-4469

Hybrid Solar Deciliation Using Tubular Solar Still Integrated with Depth and Cover Cooling

Kabeel, A. E.[1], Sharshir, S. W.[2], Abdelaziz, G. B.[3], Halim, M. A.[4] & Swidan, A.[1*]

[1]Mechanical Power Engineering Department, Faculty of Engineering, Tanta University, Tanta, EGYPT
[2]Mechanical Engineering Department, Faculty of Engineering, Kafrelsheikh University, 33516, Kafrelsheikh, EGYPT
[3]Higher Institute of Engineering and Technology, Kafrelsheikh, EGYPT
[4]Mechanical Department, Technological Faculty in Cairo, Helwan International Technological University, Cairo, EGYPT

*Corresponding Author: eng.ahmedswidan2017@gmail.com

To Cite This Article:
Kabeel, A. E., Sharshir, S. W., Abdelaziz, G. B., Halim, M. A., & Swidan, A. (2026). Hybrid Solar Deciliation Using Tubular Solar Still Integrated with Depth and Cover Cooling. *ICCCM Journal of Social Sciences and Humanities*,5 Special Issue, 82-94. https://doi.org/10.53797/icccmjssh.v5isp.10.2026

Received 19 February 2026. **Revised** 25 February 2026, **Accepted** 13 March 2026, **Available online** 25 March 2026

Abstract: Tubular solar stills (TSS) have emerged as a promising solution for freshwater production, particularly for small-scale applications in coastal and arid regions where access to reliable power sources for desalination and infrastructure for water transportation is limited. This study introduces an enhanced TSS design incorporating cover cooling to improve daily water yield. The system comprises a transparent solar tube, which maximizes solar irradiance absorption, and a black basin, which enhances heat absorption and accelerates water evaporation. The TSS was fabricated using lightweight, durable materials sourced locally to ensure cost-effectiveness and ease of deployment. Experiments were conducted to determine the optimal basin water depth (0.5 cm, 1 cm, 2 cm, and 3 cm) and cooling water flow rate (1 L/h, 2 L/h, 3 L/h, and 4 L/h). The results indicated that a lower water depth significantly enhanced performance, with a maximum productivity of 4.5 L/m² achieved at 0.5 cm depth, whereas a depth of 3 cm yielded only 3 L/m². Additionally, the optimal cooling water flow rate was found to be 2 L/h. Under these conditions, the system achieved its highest efficiency of 54.9%. Compared to a TSS without cooling, the proposed design demonstrated a 31.4% increase in water yield and a 32.6% improvement in efficiency. Furthermore, the daily thermal exergy efficiency improved by approximately 9%. From an economic perspective, the cost per liter of clean water was reduced from $0.023 in the conventional TSS to $0.019 in the modified system with cover cooling, highlighting its cost-effectiveness.

Keywords: Solar desalination, tubular solar still, water depth, cooling water flow rate, thermal performance

1. Introduction

Water scarcity is one of the most pressing global challenges, affecting both developed and developing nations due to rapid population growth, industrialization, and agricultural expansion, all while the availability of freshwater remains constant (Li et al., 2017). Approximately 97.5% of the Earth's water is saline, leaving only 2.5% as freshwater. However, the majority of this freshwater is locked in glaciers and underground reservoirs, making the accessible supply insufficient to meet the increasing global demand (Xiao et al., 2013).

To address this issue, researchers have explored various water purification technologies, with solar desalination emerging as one of the most effective and sustainable solutions (Ghaffour et al., 2015). Among these, the basin-type solar still is widely utilized due to its simple construction, cost-effectiveness, and environmentally friendly operation using solar energy (Feilizadeh et al., 2010). Despite extensive research efforts, conventional solar stills exhibit limited water production rates of approximately 2.5 L/m² per day (Kabeel et al., 2010) and relatively low efficiency, typically around 30% (Sharshir et al., 2018). Numerous advancements have been proposed to enhance the productivity and overall performance of basin-type solar stills. These include reclaiming latent heat of condensation (Sharshir et al., 2017a), incorporating graphite nanoparticles with phase change materials (PCM) (Kabeel et al., 2019a), integrating latent heat storage systems (Yousef & Hassan, 2019), and utilizing tubular solar energy collectors to improve thermal performance (Bait & Si-Ameur, 2018). Other enhancements involve implementing external and internal condensers (Rahmani &

*Corresponding author: eng.ahmedswidan2017@gmail.com

Boutriaa, 2017; Bhardwaj et al., 2016), incorporating pin fins (Rabhi et al., 2017), employing energy-storing materials (Sharshir et al., 2017b), using PCM combined with nanoparticles (Rufuss et al., 2018), and developing wick-based and stepped solar stills (Pal et al., 2018). Additionally, external and internal reflectors (Karimi Estahbanati et al., 2016), nanofluid applications Bait & Si-Ameur (2018), nanofluids combined with glass cover cooling (Sharshir et al., 2017c), and innovative absorber coatings such as TiO_2 nano black paint (Kabeel et al., 2019b) have been explored. Further advancements include integrating nanofluids with thermoelectric channels (Nazari et al., 2019), developing low-cost solar steam generators (Peng et al., 2018), incorporating wick materials (Pal et al., 2017), and combining hybrid solar still systems with humidification-dehumidification (HDH) techniques (Sharshir et al., 2016a, 2016b, 2016c).

Among these developments, tubular solar stills (TSS) have been recognized as an effective solution to address the limitations of traditional basin-type solar stills. Unlike conventional designs, TSS is a transparent cylindrical structure that allows solar irradiance to penetrate from multiple directions, maximizing energy absorption without additional components (Sharshir et al., 2019). Elashmawy (2019) experimentally demonstrated that reducing TSS tube thickness by 40% increased efficiency and freshwater yield by 13.35% and 21%, respectively, while lowering freshwater production costs by 37.5%. Similarly, Elashmawy (2017) investigated a TSS integrated with a solar tracking parabolic concentrator, reporting a remarkable 676% increase in freshwater production. Further studies have explored multi-TSS systems with linear Fresnel reflectors (Gang et al., 2019), concentric circular TSS integrated with phase change materials (Arunkumar & Kabeel, 2017), and TSS featuring corrugated basin absorbers (Elshamy & El-Said, 2018), which improved freshwater production by 26.47% compared to flat plate designs. Additionally, Arunkumar et al. (2013) developed a novel concentric TSS incorporating air and water cooling, significantly enhancing freshwater yield from 2.05 L/day (without cooling) to 5 L/day (with water cooling). Comparative studies between TSS and triangular solar stills have further confirmed the superior performance of TSS, with a 20% increase in freshwater output (Rahbar et al., 2018).

Recent innovations include vertical TSS configurations with wick materials (Hou et al., 2018), achieving a 23.9% increase in water production at reduced pressure conditions and a 17% improvement with increased ambient airflow. Additionally, vacuum-assisted TSS designs have demonstrated enhanced evaporation rates and system efficiency (Xie et al., 2018). Zanganeh et al. (2019) investigated nano-coated condensing surfaces, reporting a 23% and 86.8% increase in freshwater productivity for glass angles of 50° and 30°, respectively, compared to conventional stills. While these advancements have improved solar still performance, many modifications require additional components, increasing system complexity and costs. Furthermore, traditional designs limit solar irradiance absorption to a single direction, reducing overall energy efficiency. TSS addresses these challenges by enabling multi-directional irradiance penetration and enhanced condensation efficiency. In this study, an improved TSS design integrated with cover cooling is experimentally analyzed to optimize water production rates. The effects of varying basin water depths (0.5 cm, 1 cm, 2 cm, and 3 cm) and different cooling water flow rates (1 L/h, 2 L/h, 3 L/h, and 4 L/h) are systematically investigated. Additionally, the thermal performance of the system is assessed in terms of energy and exergy efficiencies, and the cost-effectiveness of the proposed design is evaluated. The findings contribute to the ongoing development of efficient, low-cost solar desalination systems to address global water scarcity challenges. the cost per liter of clean water was evaluated with and without cooling cover

2. Experimental Methods and Measuring Devices

2.1 Tubular Solar Still (TSS)

The Tubular Solar Still (TSS) utilized in this study is a transparent cylindrical structure made of polycarbonate, as depicted in Figures 1 and 2. This design enables solar irradiance to penetrate from all directions. The outer body of the still has a length of 100 cm, a diameter of 50 cm, and a thickness of 1.5 cm. Inside, a rectangular steel basin holds the saline water, measuring 90 cm in length, 40 cm in width, and 5 cm in and a thickness of 1.5 cm. Inside, a rectangular steel basin holds the saline water, measuring 90 cm in length, 40 cm in width, and 5 cm

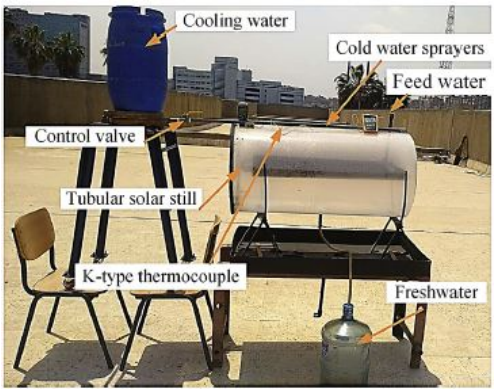

Fig. 1. Photograph of the experimental setup of tubular solar still.

in height. To enhance solar absorption and minimize reflection, the internal basin is coated in black, ensuring maximum heat absorption from the transmitted solar irradiance. As the water heats up, it evaporates, and the resulting vapor rises. Due to the temperature gradient between the vapor and the surrounding air, condensation occurs on the inner surface of the cylindrical cover. The condensed water droplets, influenced by gravity, flow downward and collect at the base of the tube as fresh distilled water. The cylindrical shape of the TSS significantly enhances water distillation efficiency by maximizing solar exposure from all angles. Moreover, compared to conventional solar stills (CSS), the water in the basin heats up more rapidly. In this study, different water depths (0.5 cm, 1 cm, 2 cm, and 3 cm) were experimentally analyzed to identify the optimal depth for efficient distillation. Once the ideal water depth was determined, various cooling water flow rates (1, 2, 3, and 4 L/h) were tested to optimize the cooling process. Temperature measurements were recorded hourly using Type-K thermocouples, monitoring key parameters such as water temperature, inlet and outlet cover temperatures, air temperature, vapor temperature, and inlet cooling water temperature.

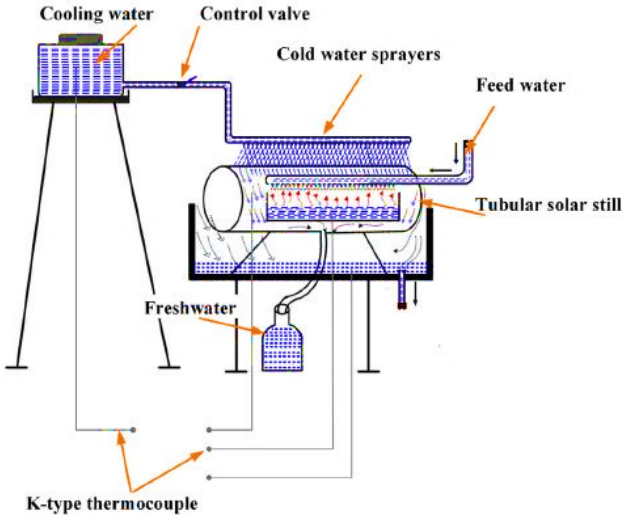

Fig. 2. Schematic diagram of the experimental setup.

2.2 The Holy Family Journey in North Egypt

During the experiment, multiple parameters were measured to ensure accuracy and reliability. The temperatures of the inner and outer glass surfaces, water, and ambient air were recorded using calibrated Type-K thermocouples, which operate within a range of 50°C to 280°C, with an uncertainty of ±0.152°C and an accuracy of ±1°C. Wind speed was measured using a digital vane-type anemometer with a measurement range of 0–45 m/s, an uncertainty of ±0.175 m/s, and an accuracy of ±1 m/s. Solar irradiance was determined using a solar meter with a range of 0–5000 W/m², an accuracy of ±5 W/m², and an uncertainty of ±2.16 W/m². Additionally, an 8-L graduated cylinder with a precision of 10 mL was used for water volume measurements, while the uncertainty of the hourly freshwater yield was approximately 3 mL. The overall uncertainty in the estimated values, which arises from the uncertainties of individual measured parameters, is referred to as uncertainty propagation. The total uncertainty of a function (X) can be calculated using the following equation: where, wx is the uncertainty of the value X, w is the uncertainty of the measured parameter and xn is the parameter of interest.

determined as follows:

$$w_x| = \sqrt{\left(\frac{\partial X}{\partial x_1}\right)^2 wx_1^2 + \left(\frac{\partial X}{\partial x_2}\right)^2 wx_2^2 + \ldots\ldots\ldots + \left(\frac{\partial X}{\partial x_n}\right)^2 wx_n^2} \quad (1)$$

3. Results and Discussion

3.1 Cinematic Conditions during the Experimental Study at Different Basin Water Depth

Climatic factors such as ambient temperature, solar irradiance, and wind speed play a crucial role in the performance of the Tubular Solar Still (TSS). The experimental study was conducted during July and August 2024

on the rooftop of the Technological Faculty in Cairo, Helwan International Technological University, Cairo, Egypt, as shown in Figure 3(a). Observations indicate that ambient temperature fluctuated between a minimum of 31°C at the beginning and end of the operation, reaching a peak of 39°C at noon. Figure 3(b) illustrates the variations in solar irradiance, which ranged from approximately 550 W/m² at 9:00 AM, peaked at 1050 W/m² at noon, and gradually decreased to around 400 W/m² by 5:00 PM. Due to consistent weather conditions, the measured values of air temperature and solar irradiance remained within a close range, as depicted in Figure 3(b). Additionally, as shown in Figure 3(c), wind speed exhibited minor fluctuations across different test days, ranging between 1.4 m/s and 4 m/s. The average climatic conditions recorded during the experimental study for different basin water depths are summarized in Table 1.

3.2 Effect of Water Depth on TSS Performance

The influence of varying water depths on the performance of the Tubular Solar Still (TSS) was analyzed by monitoring water temperature fluctuations during the experiment without cooling. Figure 4(a) illustrates the variations in water temperature at different depths (0.5 cm, 1 cm, 2 cm, and 3 cm). It is evident that water temperature follows a daily cycle, with minimum values recorded in the early morning and late evening, while the maximum temperature occurs around noon. The highest recorded water temperature was 64°C at a depth of 0.5 cm, observed at 14:00, whereas the lowest water temperature was associated with the largest water depth (3 cm), reaching a peak of only 51°C. Additionally, at 1 cm and 2 cm water depths, the maximum recorded temperatures were 61°C and 57°C, respectively. Figure 4(b) presents the variations in glass surface temperature throughout the experimental period. The tubular surface temperature ranged from a minimum of 35.7°C to a maximum of 52°C. The temperature differences between cases with different water depths were relatively small for the cover surface but significant for water temperature. As illustrated in Figure 4(b), the highest surface temperatures corresponded to the lowest water depths, as the minimal water volume required less time to heat up, leading to higher water temperatures compared to deeper water levels. Consequently, at larger water depths, the outer surface of the cover exhibited higher temperatures than at shallower depths.

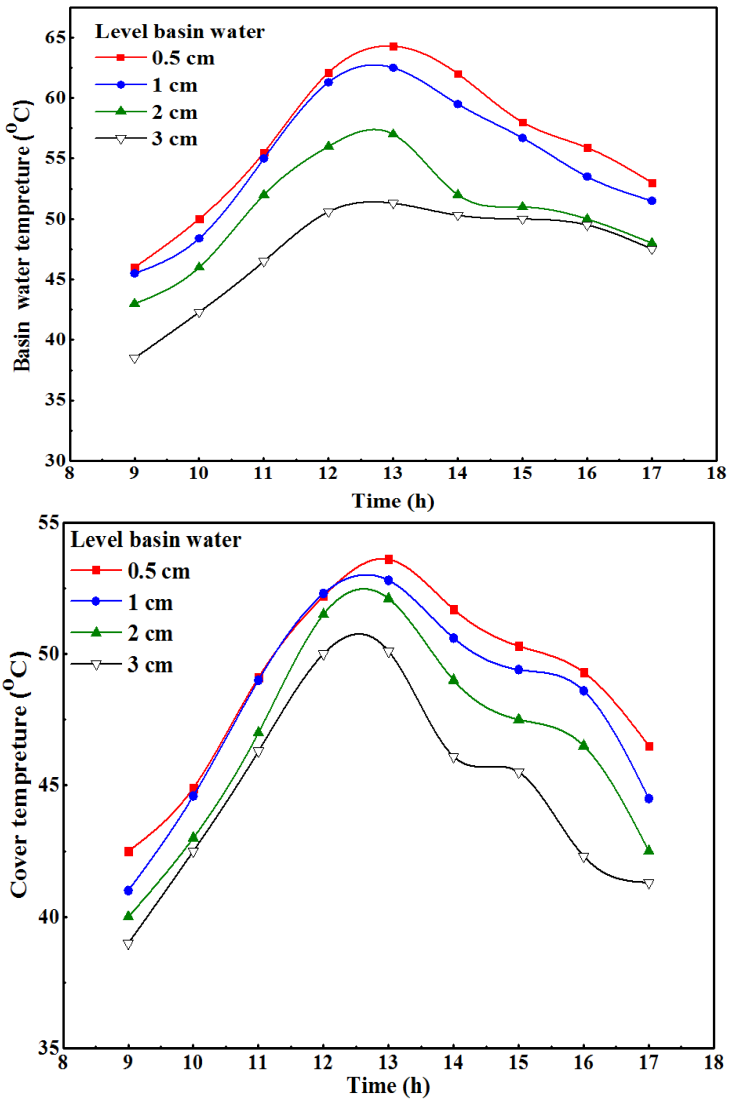

Fig. 4 Effect of different water depth on the TSS performance (a) basin water temperature, (b) cover surface temperature.

A comparison of hourly and cumulative freshwater production at different water depths is presented in Figure 5. Figure 5(a) highlights the relationship between water depth and distillate yield, demonstrating that lower water depths result in higher freshwater production. This is attributed to the reduced thermal energy required to vaporize water at shallower depths. Additionally, as previously mentioned, the temperature difference between the water and the cover surface was greater in cases of low water depth, further enhancing evaporation. The hourly freshwater output* of the TSS followed a typical pattern, starting from zero in the morning, peaking at noon, and gradually decreasing toward the evening. The maximum recorded hourly freshwater yield was 0.75, 0.7, 0.61, and 0.54 L/m² for water depths of 0.5 cm, 1 cm, 2 cm, and 3 cm, respectively. The total freshwater output over the experimental period for these respective depths was 4.45 L/m², 4.2 L/m², 3.54 L/m², and 3.09 L/m², as shown in Figure 5(b). These results indicate that water production at 0.5 cm depth was 5.95%, 25.7%, and 44% higher compared to 1 cm, 2 cm, and 3 cm depths, respectively, confirming that shallower water depths significantly enhance the distillation efficiency of the TSS.

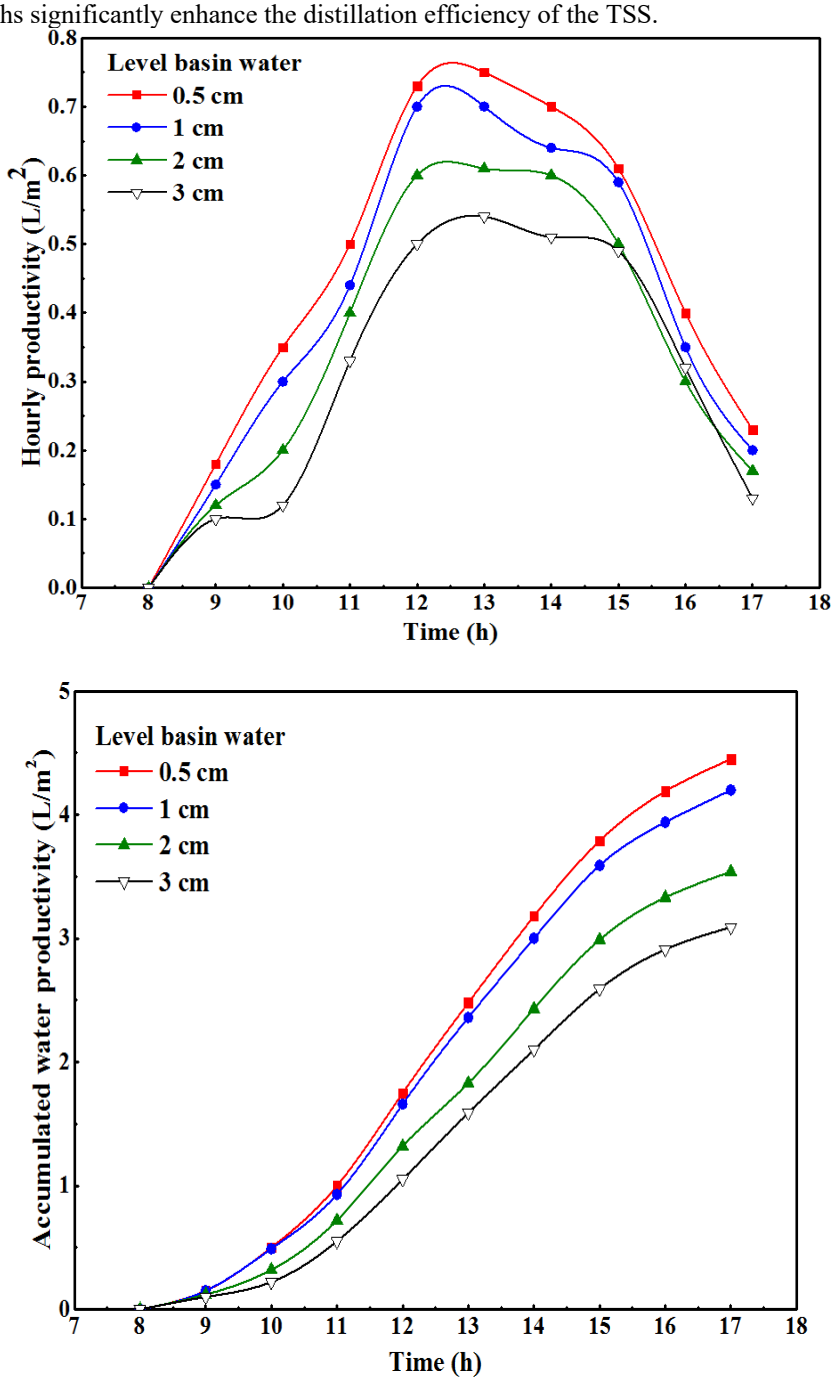

Fig. 5 Effect of different water depth on the TSS performance (a) freshwater output per hour (b) total freshwater per day

3.3 Climate Conditions during the Cooling Water Flow Over the Cover

The weather conditions observed during the cooling water flow over the cover at varying flow rates are presented in Figure 6. Air Temperature Analysis. As shown in Figure 6(a), the air temperatures recorded over the four experimental

days remained nearly identical, with only minor variations. These negligible differences indicate that ambient temperature had a minimal impact on the comparative analysis of different cooling water flow rates. Solar Irradiance Trends. Figure 6(b) illustrates the solar irradiance patterns recorded during the selected test days. The data confirm that solar intensity followed a consistent pattern across all days, reflecting the stability of weather conditions during the experimental period. The solar irradiance exhibited its lowest values during early morning and late evening, reaching a peak of 1050 W/m² at noon before gradually declining toward sunset. Wind Speed Variations. The wind speed fluctuations during the experimental period are depicted in Figure 6(c). Similar to air temperature and solar irradiance, wind speed did not show significant variation between different test days. The recorded wind speed ranged between 0.8 m/s and 3.6 m/s, further validating the consistency of climatic conditions throughout the study. A summary of the average climatic conditions observed during the experimental period under varying cooling water flow rates is provided in Table 2. These stable environmental conditions ensure that any variations in the system's performance can be attributed primarily to the effect of different water-cooling flow rates rather than external climatic influences.

Table 2 The average weather conditions during cover cooling at different water flow rates

Experiment day	Average solar intensity, (W/m^2)	Average air temperature, (°C)	Average wind speed, (m/s)
20-07-2024	766	34.8	2.6
25-07-2024	782	34.7	2.4
01-08-2024	772	35.77	2
10-05-2024	773	34.3	2.3

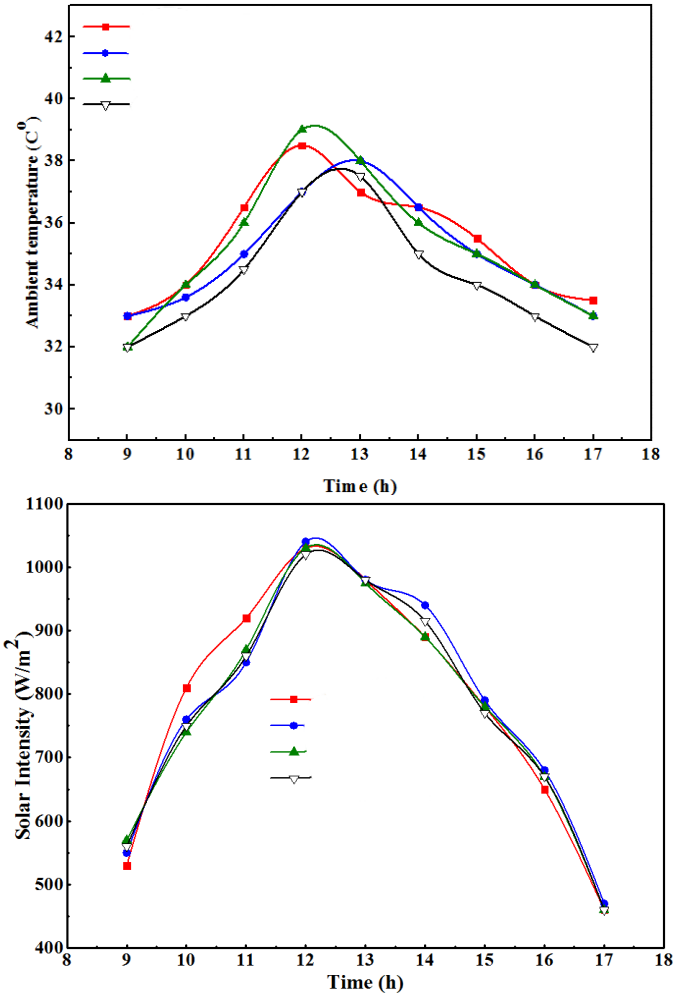

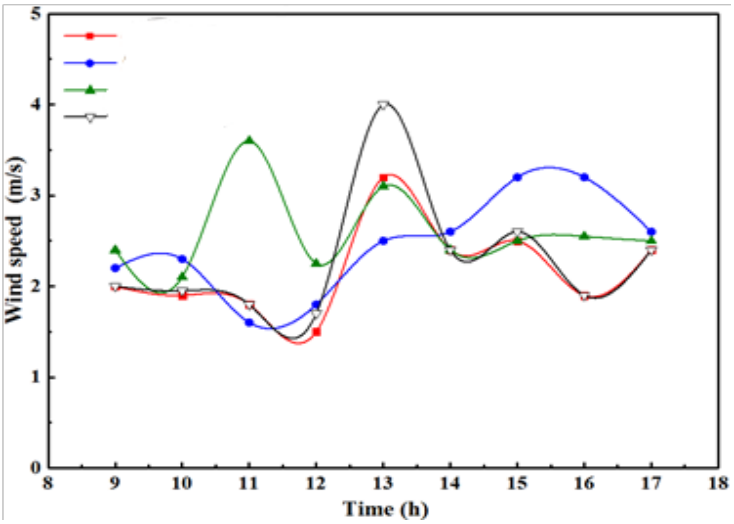

Fig. 6 Weather conditions during the experimental study (a) ambient temperature, (b) solar irradiance, and (c) wind speed.

3.4 Performance of TSS with Water Cooling Over the Cover

Cold-Water Temperature Trends. The variation in *cold-water temperature over the condensing cover during the experimental days is depicted in Figure 7(a). The temperature fluctuated within a narrow range, starting at 29°C in the morning, peaking at 34°C at noon, and eventually settling at 30°C by the end of the day. Water Basin Temperature Behavior. Figure 7(b) presents the temperature variations in the. TSS water basin over time under different cooling water flow rates (1, 2, 3, and 4 L/h). Across all cases, the water temperature followed a consistent pattern starting from its lowest value in the morning, increasing to its peak at noon, and then gradually declining toward the evening. The highest basin water temperature was recorded at 60°C for 1 L/h, followed by 56°C for 2 L/h, while the lowest temperatures were observed at 3 L/h (51°C) and 4 L/h (49.6°C). This trend highlights that higher cooling flow rates effectively absorb more heat from the cover, thereby reducing heat transfer inside the TSS. Additionally, excessive cooling flow rates may obstruct solar irradiance penetration into the system. Cover Temperature Variations. The cover temperature at different water cooling flow rates is illustrated in Figure 7(c). It was observed that lower cooling water flow rates resulted in higher cover temperatures, while higher flow rates led to lower cover temperatures. The cover temperature ranged from 30°C to a maximum of 50°C at noon. Freshwater Production Efficiency the hourly freshwater output for different cooling water flow rates (1, 2, 3, and 4 L/h) is shown in Figure 8(a). In all cases, water production started from zero in the morning, peaked at noon, and then gradually declined toward the evening. The results indicate that the optimal cooling flow rates for maximizing freshwater production were 2 L/h and 3 L/h, yielding maximum hourly outputs of 0.93 L/m² and 0.88 L/m² at 13:00, respectively. These rates provided the best balance between effective heat removal and sufficient temperature difference between the basin water and the cover. Conversely, at 1 L/h, the cooling effect was insufficient to condense a significant amount of water due to the smaller temperature difference, leading to an hourly production of 0.86 L/m². Meanwhile, at 4 L/h, the excessive cooling water layer on the glass reduced solar radiation absorption, limiting the hourly production to 0.84 L/m². Total Freshwater Yield. The total freshwater output at different cooling water flow rates is presented in Figure 8(b). The production values were:

- 1 L/h → 5.42 L/m² - 2 L/h → 5.85 L/m²
- 3 L/h → 5.53 L/m² - 4 L/h → 5.23 L/m²

These results indicate that using 2 L/h cooling water improved freshwater production by approximately 7.93%, 5.8%, and 11.8% compared to 1 L/h, 3 L/h, and 4 L/h, respectively. Effect of Cooling on Thermal Performance. The condensation cover* absorbs heat from vapor condensation on its internal surface and dissipates it to the ambient environment through convection and radiation (Omara et al., 2017). However, at low air velocity, these heat dissipation mechanisms are limited, resulting in high cover temperatures and a small temperature difference between the water and the condensation cover, which reduces thermal performance. To enhance performance, cover cooling was implemented. By continuously supplying cold water over the condensation cover, its temperature was reduced, thereby increasing the temperature difference and enhancing vaporization rates. Cooling is also crucial for self-cleaning the condensation surface, further optimizing system efficiency. Moreover, the tubular configuration of the TSS cover provides a larger cooling surface area compared to conventional basin stills, making water cooling significantly more effective in enhancing thermal performance. Importantly, the applied cooling water flow was maintained at an optimal level to avoid obstructing solar radiation penetration, ensuring maximum efficiency.

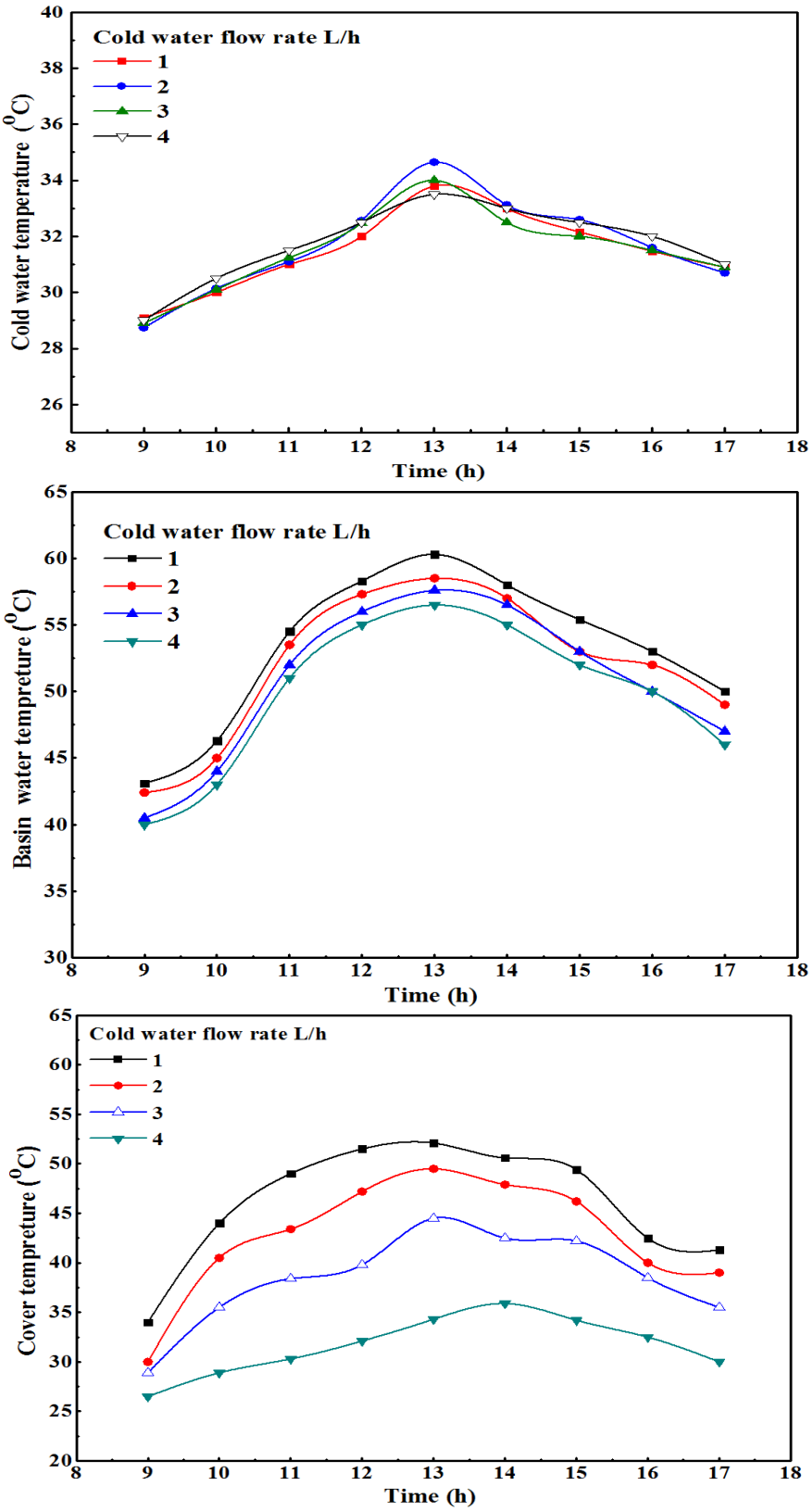

Fig. 7 Performance of the TSS with cover cooling (a) cold-water temperature, (b) basin water temperature, and (c) cover temperature.

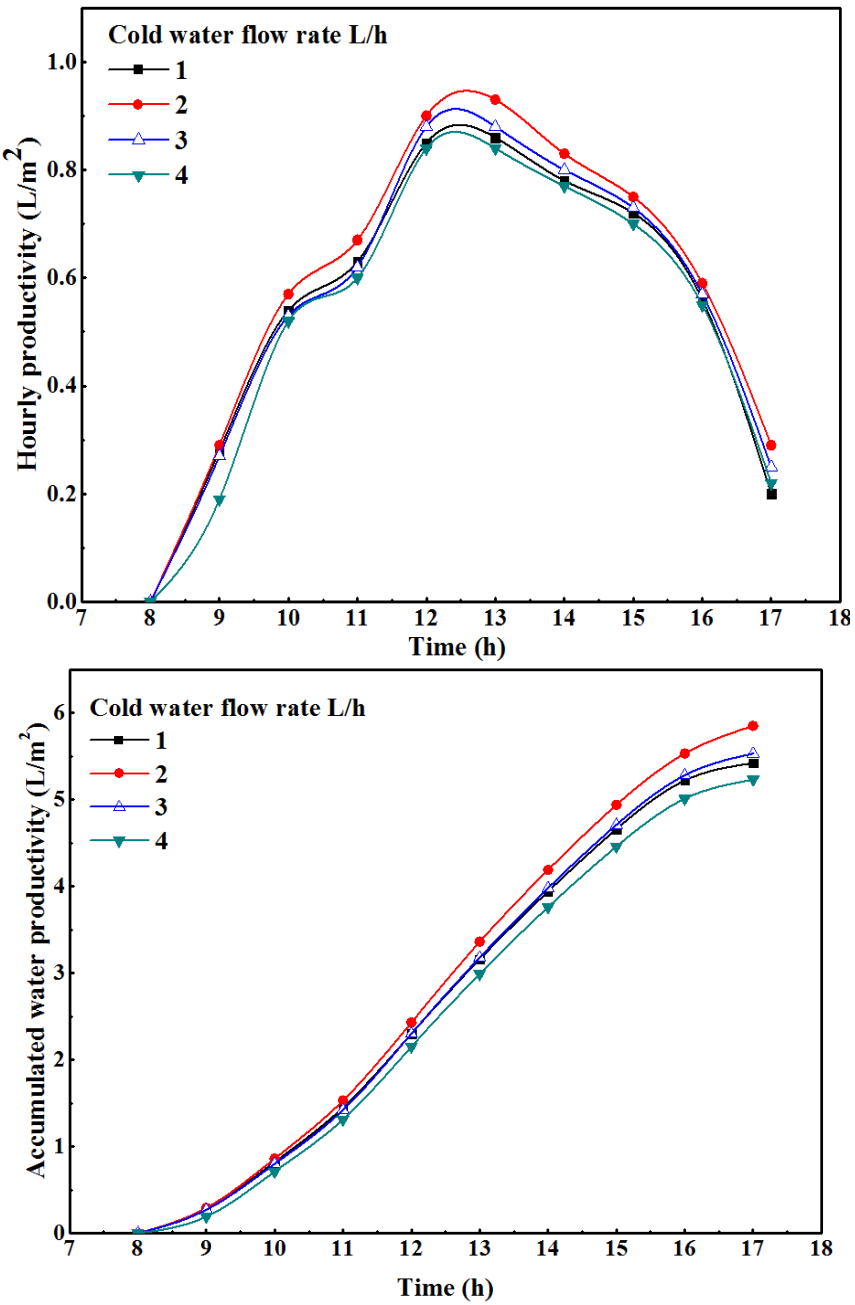

Fig. 8 Performance of the TSS with cover cooling (a) hourly productivity and (b) accumulated productivity.

3.5 Thermal Efficiency of Tubular Solar Still

The daily thermal efficiency (ηd) is defined as the ratio of the total hourly freshwater yield ($mdis$) multiplied by the evaporation enthalpy change (lfg) to the total solar irradiance ($I(t)$) absorbed by the total absorber area (Abs), as expressed in the following equation:

$$\eta_d = \frac{\sum m_{dis} \times \lambda_{fg}}{\sum I(t) \times A_{bs} \times 3600} \quad (2)$$

The evaporation enthalpy change is calculated at the average water basin temperature (Tbw) using the equation provided by Kabeel and Abdelgaied (2017):

$$\lambda_{fg} = 10^3 \times [2501.9 - 2.40706 \times T_{bw} + 1.192217 \times 10^{-3} \times T_{bw}^2 - 1.5863 \times 10^{-5}] \quad (3)$$

Where (**λfg**) represents the evaporation enthalpy change (J/kg). The results indicate that the TSS efficiency without cover cooling was approximately 41.4% at a water depth of 0.5 cm. This efficiency is considered satisfactory compared to the conventional solar still (CSS), which has an efficiency of 30% (Sharshir et al., 2017c). Furthermore, with optimal cover cooling at 2 L/h* and 0.5 cm water depth, the TSS efficiency increased to 54.9%, marking an improvement of 32.6%* due to the cooling effect.

3.6 Exergy Efficiency of Tubular Solar Stil

Exergy analysis is used to evaluate the quality of energy within thermal systems. The exergy efficiency (ηEX) of the solar distiller is defined as the ratio of output exergy to input exergy (Elango et al., 2015):

$$\eta_{EX} = \frac{\text{Output Exergy}}{\text{Input Exergy}} = \frac{E_{x_{evap}}}{E_{x_{input}}} \quad (4)$$

The output exergy is a function of the freshwater output from the distiller and is given by (Zoori et al., 2013; Elango et al., 2015; Vaithilingam & Esakkimuthu, 2015):

$$E_{x_{output}} = E_{x_{evap}} = \frac{m_{dis} \times \lambda_{fg}}{\left(3600 s.h^{-1}\right)} \times \left(1 - \frac{T_a + 273.15}{T_{bw} + 273.15}\right) \quad (5)$$

The input exergy (ηEX) is derived as a function of solar insolation (Elango et al., 2015):

$$E_{x_{sun}} = A_{bs} \times I(t)_s \left[1 - \frac{4}{3} \times \left(\frac{T_a + 273.15}{T_s}\right) + \frac{1}{3} \times \left(\frac{T_a + 273.15}{T_s}\right)^4\right] \quad (6)$$

The results indicate that the daily exergy efficiency for TSS with and without cover cooling was 3.65% and 3.35%, respectively. This suggests that cover cooling enhances the exergy efficiency by approximately 9%.

4. Economic Analysis

The economic aspect is a critical factor in determining the effectiveness of different desalination systems. This section presents the financial evaluation of the proposed TSS. Various factors influence the production cost of the TSS desalination unit, including site location, unit size, product water demand, feed water characteristics, availability of skilled personnel, and required water qualiy. A key financial advantage of TSS desalination is its simple design, installation, operation, and maintenance, requiring minimal infrastructure. The goal is to minimize costs while ensuring efficiency. The total cost (fixed and operational) of TSS can be estimated as follows: Table 3.

Table 3 Cost data of TSS components

Cost ($)	TSS without cooling	TSS with
Transparent cylinder	100	100
Pipes and valves	5	10
Black basin	30	30
Cold water tank	-	5
Silicon and paints	15	15
Manufacture	100	100
Total fixed cost (F)	250	260

4.1 Total Cost Estimation of TSS

The CPL from TSS can be calculated based on yearly productivity (Sharshir et al., 2018) as in Eq. (7).

$$CPL = C / TFP \quad (7)$$

where:

C=total cost, determined by: where, C is the total cost and can be determine from Eq. (8) whileTFP is the total freshwater during the life span and is expressed by Eq. (8).

$$C = V + F \quad (8)$$

by:

$$TFP = \text{Yearly productivity} \times n \quad (9)$$

where, n is the expected still lifetime and was assumed 10 years.

The yearly productivity can be calculated as follows:

$$\text{Yearly productivity} = m \times \text{operating days} \quad (10)$$

Operating days = 340 sunny days per year. Based on cost analysis, the cost per liter (CPL) of freshwater from TSS with and without cover cooling was \$0.019 and \$0.023, respectively. These results confirm that TSS with cover cooling offers lower production costs compared to TSS without cooling. Additionally, a comparative analysis of TSS and CSS in terms of freshwater productivity, system efficiency, and CPL demonstrates that TSS achieves higher efficiency, greater freshwater output, and lower production costs than CSS.

5. Conclusion

The growing demand for clean and sustainable energy has positioned solar energy as an eco-friendly and cost-effective solution for water desalination. This study focuses on the design, operation, and performance evaluation of Tubular Solar Stills (TSS) as a zero-emission and economically viable method for freshwater production in coastal and arid regions. Experiments were conducted under the climatic conditions of Cairo, Egypt, to analyze the impact of various water depths and cover cooling flow rates on TSS performance. The key findings are summarized as follows:

a. Freshwater production at 1 cm, 2 cm, and 3 cm water depths without cooling was 4.2 L/m², 3.54 L/m², and 3.09 L/m², respectively.
b. The maximum freshwater production without cooling was 4.5 L/m², achieved at the lowest water depth of 0.5 cm.
c. Under cooling conditions with different flow rates (1 L/h, 3 L/h, and 4 L/h), the freshwater production was 5.42 L/m², 5.53 L/m², and 5.23 L/m², respectively.
d. The optimal combination of 0.5 cm water depth and 2 L/h cooling flow rate yielded the highest freshwater production of 5.85 L/m².
e. With the optimal water depth and no cooling, the daily efficiency was 41.4%, whereas, under optimal conditions with cooling, the efficiency increased to 54.9%.
f. The daily thermal exergy efficiency for TSS with and without cover cooling was 3.65% and 3.35%, respectively.
g. Economic analysis confirmed that CPL of freshwater under optimal conditions was \$0.019, compared to \$0.023 without cooling , making TSS a cost-effective desalination solution. These findings highlight the significant performance improvements and cost benefits of using cover cooling in TSS, demonstrating its superiority over conventional solar stills (CSS) in terms of efficiency, freshwater output, and economic feasibility.

Acknowledgement

The authors would like to express their sincere gratitude to all respondents who willingly participated in this study and provided valuable data. Their cooperation and honesty greatly contributed to the completion and quality of this research. The authors would also like to thank all co-authors for their valuable collaboration and contribution in completing this manuscript.

Conflict of Interest

The authors declare no conflicts of interest

References

Arunkumar, T., & Kabeel, A. E. (2017). Effect of phase change material on concentric circular tubular solar still-Integration meets enhancement. Desalination, 414, 46-50. https://doi.org/10.1016/j.desal.2017.03.035

Arunkumar, T., Jayaprakash, R., Ahsan, A., Denkenberger, D., & Okundamiya, M. S. (2013). Effect of water and air flow on concentric tubular solar water desalting system. *Applied energy*, *103*, 109-115. https://doi.org/10.1016/j.apenergy.2012.09.014

Bait, O., & Si–Ameur, M. (2018). Enhanced heat and mass transfer in solar stills using nanofluids: a review. Solar Energy, 170, 694-722. https://doi.org/10.1016/j.solener.2018.06.020

Bhardwaj, R., Ten Kortenaar, M. V., & Mudde, R. F. (2016). Inflatable plastic solar still with passive condenser for single family use. Desalination, 398, 151-156. https://doi.org/10.1016/j.desal.2016.07.011

Elashmawy, M. (2017). An experimental investigation of a parabolic concentrator solar tracking system integrated with a tubular solar still. Desalination, 411, 1-8. https://doi.org/10.1016/j.desal.2017.02.003

Elashmawy, M. (2019). Effect of surface cooling and tube thickness on the performance of a high temperature standalone tubular solar still. Applied Thermal Engineering, 156, 276-286. https://doi.org/10.1016/j.applthermaleng.2019.04.068

Elshamy, S. M., & El-Said, E. M. (2018). Comparative study based on thermal, exergetic and economic analyses of a tubular solar still with semi-circular corrugated absorber. Journal of cleaner production, 195, 328-339. https://doi.org/10.1016/j.jclepro.2018.05.243

Elango, C., Gunasekaran, N., & Sampathkumar, K. (2015). Thermal models of solar still—A comprehensive review. Renewable and Sustainable Energy Reviews, 47, 856-911. https://doi.org/10.1016/j.rser.2015.03.054

Estahbanati, M. K., Ahsan, A., Feilizadeh, M., Jafarpur, K., Ashrafmansouri, S. S., & Feilizadeh, M. (2016). Theoretical and experimental investigation on internal reflectors in a single-slope solar still. Applied energy, 165, 537-547. https://doi.org/10.1016/j.apenergy.2015.12.047

Feilizadeh, M., Soltanieh, M., Jafarpur, K., & Estahbanati, M. K. (2010). A new radiation model for a single-slope solar still. Desalination, 262(1-3), 166-173. https://doi.org/10.1016/j.desal.2010.06.005

Gang, W., Qichang, Y., Hongfei, Z., Yi, Z., Hui, F., & Rihui, J. (2019). Direct utilization of solar linear Fresnel reflector on multi-effect eccentric horizontal tubular still with falling film. Energy, 170, 170-184. https://doi.org/10.1016/j.energy.2018.12.150

Ghaffour, N., Bundschuh, J., Mahmoudi, H., & Goosen, M. F. (2015). Renewable energy-driven desalination technologies: A comprehensive review on challenges and potential applications of integrated systems. Desalination, 356, 94-114. https://doi.org/10.1016/j.desal.2014.10.024

Hou, J., Yang, J., Chang, Z., Zheng, H., & Su, Y. (2018). The mass transfer coefficient assessment and productivity enhancement of a vertical tubular solar brackish water still. Applied Thermal Engineering, 128, 1446-1455. https://doi.org/10.1016/j.applthermaleng.2017.09.129

Kabeel, A. E., Hamed, A. M., & El-Agouz, S. A. (2010). Cost analysis of different solar still configurations. Energy, 35(7), 2901-2908. https://doi.org/10.1016/j.energy.2010.03.021

Kabeel, A. E., & Abdelgaied, M. (2017). Observational study of modified solar still coupled with oil serpentine loop from cylindrical parabolic concentrator and phase changing material under basin. Solar Energy, 144, 71-78. https://doi.org/10.1016/j.solener.2017.01.007

Kabeel, A. E., Abdelgaied, M., & Eisa, A. (2019). Effect of graphite mass concentrations in a mixture of graphite nanoparticles and paraffin wax as hybrid storage materials on performances of solar still. Renewable Energy, 132, 119-128. https://doi.org/10.1016/j.renene.2018.07.147

Kabeel, A. E., Sathyamurthy, R., Sharshir, S. W., Muthumanokar, A., Panchal, H., Prakash, N., ... & El Kady, M. S. (2019). Effect of water depth on a novel absorber plate of pyramid solar still coated with TiO2 nano black paint. Journal of cleaner production, 213, 185-191. https://doi.org/10.1016/j.jclepro.2018.12.185

Li, Y., Gao, T., Yang, Z., Chen, C., Kuang, Y., Song, J., ... & Hu, L. (2017). Graphene oxide-based evaporator with one-dimensional water transport enabling high-efficiency solar desalination. Nano Energy, 41, 201-209. https://doi.org/10.1016/j.nanoen.2017.09.034

Nazari, S., Safarzadeh, H., & Bahiraei, M. (2019). Experimental and analytical investigations of productivity, energy and exergy efficiency of a single slope solar still enhanced with thermoelectric channel and nanofluid. Renewable energy, 135, 729-744. https://doi.org/10.1016/j.renene.2018.12.059

Omara, Z. M., Abdullah, A. S., Kabeel, A. E., & Essa, F. A. (2017). The cooling techniques of the solar stills' glass covers–A review. Renewable and Sustainable Energy Reviews, 78, 176-193. https://doi.org/10.1016/j.rser.2017.04.085

Pal, P., Yadav, P., Dev, R., & Singh, D. (2017). Performance analysis of modified basin type double slope multi–wick solar still. Desalination, 422, 68-82. https://doi.org/10.1016/j.desal.2017.08.009

Pal, P., Dev, R., Singh, D., & Ahsan, A. (2018). Energy matrices, exergoeconomic and enviroeconomic analysis of modified multi–wick basin type double slope solar still. Desalination, 447, 55-73. https://doi.org/10.1016/j.desal.2018.09.006

Peng, G., Ding, H., Sharshir, S. W., Li, X., Liu, H., Ma, D., ... & Yang, N. (2018). Low-cost high-efficiency solar steam generator by combining thin film evaporation and heat localization: Both experimental and theoretical study. Applied Thermal Engineering, 143, 1079-1084. https://doi.org/10.1016/j.applthermaleng.2018.08.004

Rabhi, K., Nciri, R., Nasri, F., Ali, C., & Bacha, H. B. (2017). Experimental performance analysis of a modified single-basin single-slope solar still with pin fins absorber and condenser. Desalination, 416, 86-93. https://doi.org/10.1016/j.desal.2017.04.023

Rahbar, N., Asadi, A., & Fotouhi-Bafghi, E. (2018). Performance evaluation of two solar stills of different geometries: tubular versus triangular: experimental study, numerical simulation, and second law analysis. Desalination, 443, 44-55. https://doi.org/10.1016/j.desal.2018.05.015

Rahmani, A., & Boutriaa, A. (2017). Numerical and experimental study of a passive solar still integrated with an external condenser. international journal of hydrogen energy, 42(48), 29047-29055. https://doi.org/10.1016/j.ijhydene.2017.07.242

Rufuss, D. D. W., Suganthi, L., Iniyan, S., & Davies, P. A. (2018). Effects of nanoparticle-enhanced phase change material (NPCM) on solar still productivity. Journal of Cleaner Production, 192, 9-29. https://doi.org/10.1016/j.jclepro.2018.04.201

Sharshir, S. W., El-Samadony, M. O. A., Peng, G., Yang, N., Essa, F. A., Hamed, M. H., & Kabeel, A. E. (2016). Performance enhancement of wick solar still using rejected water from humidification-dehumidification unit and film cooling. Applied Thermal Engineering, 108, 1268-1278. https://doi.org/10.1016/j.applthermaleng.2016.07.179

Sharshir, S. W., Elsheikh, A. H., Peng, G., Yang, N., El-Samadony, M. O. A., & Kabeel, A. E. (2017). Thermal performance and exergy analysis of solar stills–A review. Renewable and Sustainable Energy Reviews, 73, 521-544. https://doi.org/10.1016/j.rser.2017.01.156

Sharshir, S. W., Peng, G., Yang, N., El-Samadony, M. O. A., & Kabeel, A. E. (2016). A continuous desalination system using humidification–dehumidification and a solar still with an evacuated solar water heater. Applied Thermal Engineering, 104, 734-742. https://doi.org/10.1016/j.applthermaleng.2016.05.120

Sharshir, S. W., Peng, G., Yang, N., Eltawil, M. A., Ali, M. K. A., & Kabeel, A. E. (2016). A hybrid desalination system using humidification-dehumidification and solar stills integrated with evacuated solar water heater. Energy conversion and management, 124, 287-296. https://doi.org/10.1016/j.enconman.2016.07.028

Sharshir, S. W., Peng, G., Wu, L., Essa, F. A., Kabeel, A. E., & Yang, N. (2017). The effects of flake graphite nanoparticles, phase change material, and film cooling on the solar still performance. Applied energy, 191, 358-366. https://doi.org/10.1016/j.apenergy.2017.01.067

Sharshir, S. W., Peng, G., Wu, L., Yang, N., Essa, F. A., Elsheikh, A. H., ... & Kabeel, A. E. (2017). Enhancing the solar still performance using nanofluids and glass cover cooling: experimental study. Applied thermal engineering, 113, 684-693. https://doi.org/10.1016/j.applthermaleng.2016.11.085

Sharshir, S. W., Peng, G., Elsheikh, A. H., Edreis, E. M., Eltawil, M. A., Abdelhamid, T., ... & Yang, N. (2018). Energy and exergy analysis of solar stills with micro/nano particles: a comparative study. Energy conversion and management, 177, 363-375. https://doi.org/10.1016/j.enconman.2018.09.074

Sharshir, S. W., Ellakany, Y. M., Algazzar, A. M., Elsheikh, A. H., Elkadeem, M. R., Edreis, E. M., ... & Elashry, M. S. (2019). A mini review of techniques used to improve the tubular solar still performance for solar water desalination. Process Safety and Environmental Protection, 124, 204-212. https://doi.org/10.1016/j.psep.2019.02.020

Vaithilingam, S., & Esakkimuthu, G. S. (2015). Energy and exergy analysis of single slope passive solar still: an experimental investigation. Desalination and Water Treatment, 55(6), 1433-1444. https://doi.org/10.1080/19443994.2014.928794

Xiao, G., Wang, X., Ni, M., Wang, F., Zhu, W., Luo, Z., & Cen, K. (2013). A review on solar stills for brine desalination. Applied Energy, 103, 642-652. https://doi.org/10.1016/j.apenergy.2012.10.029

Xie, G., Sun, L., Yan, T., Tang, J., Bao, J., & Du, M. (2018). Model development and experimental verification for tubular solar still operating under vacuum condition. Energy, 157, 115-130. https://doi.org/10.1016/j.energy.2018.05.130

Yousef, M. S., & Hassan, H. (2019). An experimental work on the performance of single slope solar still incorporated with latent heat storage system in hot climate conditions. Journal of cleaner production, 209, 1396-1410. https://doi.org/10.1016/j.jclepro.2018.11.120

Zanganeh, P., Goharrizi, A. S., Ayatollahi, S., & Feilizadeh, M. (2019). Productivity enhancement of solar stills by nano-coating of condensing surface. Desalination, 454, 1-9. https://doi.org/10.1016/j.desal.2018.12.007

Zoori, H. A., Tabrizi, F. F., Sarhaddi, F., & Heshmatnezhad, F. (2013). Comparison between energy and exergy efficiencies in a weir type cascade solar still. Desalination, 325, 113-121. https://doi.org/10.1016/j.desal.2013.07.004